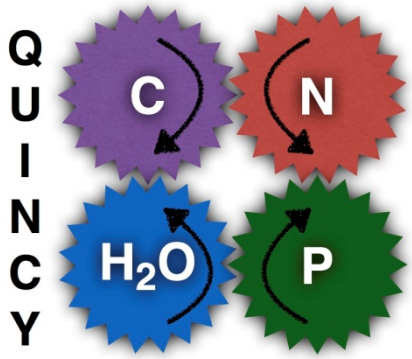

The response of ecosystem water-use efficiency to rising atmospheric CO2 concentrations: sensitivity and large-scale biogeochemical implications

Final version

(with Permission and Acknowledgement to New Phytologist
Dec. 16., 2016)

Knauer, J., Zaehle, S., Reichstein, M., Medlyn, B. E., Forkel, M., Hagemann, S., Werner, C.

Published in: New Phytologist

Reference: Knauer, J., Zaehle, S., Reichstein, M., Medlyn, B. E., Forkel, M., Hagemann, S., et al. (2017). The response of ecosystem water-use efficiency to rising atmospheric CO2 concentrations: sensitivity and large-scale biogeochemical implications. New Phytologist, 213(4), 1654-1666. doi:10.1111/nph.14288.

This project has received funding from the European Union's Horizon 2020 research and innovation programme under grant agreement No 647204

Research

New Phytologist

The response of ecosystem water-use efficiency to rising atmospheric CO_2 concentrations: sensitivity and large-scale biogeochemical implications

Jürgen Knauer[1,2], Sönke Zaehle[1,3], Markus Reichstein[1,3], Belinda E. Medlyn[4], Matthias Forkel[1,5], Stefan Hagemann[6] and Christiane Werner[7]

[1]Department of Biogeochemical Integration, Max Planck Institute for Biogeochemistry, 07745 Jena, Germany; [2]International Max Planck Research School for Global Biogeochemical Cycles (IMPRS-gBGC), 07745 Jena, Germany; [3]Michael-Stifel-Center Jena for Data-Driven and Simulation Science, 07745 Jena, Germany; [4]Hawkesbury Institute for the Environment, Western Sydney University, Richmond, NSW 2753, Australia; [5]Remote Sensing Research Group, Department of Geodesy and Geoinformation, Technische Universität Wien, 1040 Vienna, Austria; [6]Max Planck Institute for Meteorology, 20146 Hamburg, Germany; [7]Department of Ecosystem Physiology, University of Freiburg, 79085 Freiburg, Germany

Author for correspondence:
Jürgen Knauer
Tel.: +49 3641 576234
Email: jknauer@bgc-jena.mpg.de

Received: *16 July 2016*
Accepted: *17 September 2016*

New Phytologist (2017) **213:** 1654–1666
doi: 10.1111/nph.14288

Key words: continental discharge, evapotranspiration, leaf to ecosystem scaling, rising atmospheric CO_2 concentration, seasonal CO_2 exchange, water-use efficiency (WUE).

Summary

- Ecosystem water-use efficiency (WUE) is an important metric linking the global land carbon and water cycles. Eddy covariance-based estimates of WUE in temperate/boreal forests have recently been found to show a strong and unexpected increase over the 1992–2010 period, which has been attributed to the effects of rising atmospheric CO_2 concentrations on plant physiology.
- To test this hypothesis, we forced the observed trend in the process-based land surface model JSBACH by increasing the sensitivity of stomatal conductance (g_s) to atmospheric CO_2 concentration. We compared the simulated continental discharge, evapotranspiration (ET), and the seasonal CO_2 exchange with observations across the extratropical northern hemisphere.
- The increased simulated WUE led to substantial changes in surface hydrology at the continental scale, including a significant decrease in ET and a significant increase in continental runoff, both of which are inconsistent with large-scale observations. The simulated seasonal amplitude of atmospheric CO_2 decreased over time, in contrast to the observed upward trend across ground-based measurement sites.
- Our results provide strong indications that the recent, large-scale WUE trend is considerably smaller than that estimated for these forest ecosystems. They emphasize the decreasing CO_2 sensitivity of WUE with increasing scale, which affects the physiological interpretation of changes in ecosystem WUE.

Introduction

The ongoing rise in atmospheric CO_2 concentration (c_a) affects gas exchange between the vegetation and the atmosphere. Plants respond directly to rising c_a through increased net carbon assimilation (A_n) and reduced stomatal conductance (g_s) (Morison, 1987; Field *et al.*, 1995; Ainsworth & Rogers, 2007). These fundamental physiological responses lead to increased intrinsic water-use efficiency (iWUE = A_n/g_s) and reduced transpiration (T) at the leaf level, with potential implications for the terrestrial hydrological cycle and global climate (Sellers *et al.*, 1996; Betts *et al.*, 2007; Doutriaux-Boucher *et al.*, 2009; Andrews *et al.*, 2011). Current theory predicts a moderate decrease in g_s as CO_2 concentrations rise, which results in an approximately proportional increase of iWUE with c_a, and a constant ratio of intercellular (c_i) to ambient CO_2 concentrations (c_i/c_a) (Ball *et al.*, 1987; Leuning, 1995; Katul *et al.*, 2010; Medlyn *et al.*, 2011).

These theoretical considerations are strongly supported by multiple lines of experimental and observational evidence at the leaf, plant, and stand level. Reconstructed long-term records of c_i using tree-ring carbon isotope ($\delta^{13}C$) measurements suggest a moderate increase in iWUE of 20.5% from the 1960s to the early 2000s with a consistent response among climate zones and biomes (Peñuelas *et al.*, 2011). The same method applied to temperate and boreal forests over the 20th century has similarly shown an approximately proportional increase of iWUE and c_a (Feng, 1999; Saurer *et al.*, 2014; Frank *et al.*, 2015), with some sites showing a weakened iWUE response to c_a towards the end of the 20th century (Waterhouse *et al.*, 2004; Gagen *et al.*, 2011). Exposing plants to elevated CO_2 concentrations yields similar physiological responses. Results from three free-air CO_2 enrichment (FACE) experiments demonstrated that C3 plants growing in CO_2-enriched air (ambient CO_2 + 200 ppm; *c.* 50% increase in c_a) showed concurrent significant reductions in g_s and increases

in photosynthesis, which resulted in an increase of 68% in iWUE, and an unchanged c_i/c_a (Ainsworth & Long, 2005).

Intrinsic WUE is an important metric at leaf level, characterizing plant physiological properties irrespective of atmospheric water demand (Ehleringer *et al.*, 1993). At the ecosystem level, WUE can be approximated by the ratio of gross primary production (GPP) to evapotranspiration (ET) under conditions of low nonbiotic components of the evaporation flux, such as soil or interception evaporation. As ecosystem WUE is strongly modulated by climatic factors, in particular vapor pressure deficit (VPD), an 'inherent' WUE metric (IWUE = (GPP × VPD)/ET) was defined to facilitate the comparison of ecosystems with different atmospheric demand and to provide an approximation of iWUE at the ecosystem level (Beer *et al.*, 2009). IWUE, as all other WUE metrics at the ecosystem level, is subject to environmental feedbacks, which tend to strengthen as scale is increased (Field *et al.*, 1995; Wilson *et al.*, 1999). In particular, the partial decoupling of canopies from the atmosphere makes stand transpiration become increasingly insensitive to changes in canopy conductance (G_c) (Jarvis & McNaughton, 1986), and a given decrease in G_c has been shown to translate into a weaker response of transpiration, even in relatively well coupled forests (e.g. Wullschleger *et al.*, 2002). Elevated c_a further has structural effects on plant canopies through increasing leaf area index (LAI) (Norby & Zak, 2011), which has been surmised to reduce or even offset the physiological effects of c_a on vegetation water use (Piao *et al.*, 2007; Gerten *et al.*, 2008). Consequently, transpiration and WUE at the ecosystem level are less responsive to changes in c_a than their leaf-level equivalents (Wilson *et al.*, 1999; Wullschleger *et al.*, 2002; De Kauwe *et al.*, 2013).

Notwithstanding these expectations, a recent analysis of eddy covariance data from 21 flux tower sites across temperate and boreal forests from 1992 to 2010 (Keenan *et al.*, 2013; henceforth 'K13') showed a strong increase in ecosystem IWUE. This study attributed the trend in IWUE to vegetation responses to rising atmospheric CO_2 concentrations, but the observed increase was substantially stronger than predicted by current theory and found by previous empirical evidence. The hypothesis put forward was that plant gas exchange is regulated in a way to keep c_i constant despite continuously increasing c_a, which suggests that the most likely underlying physiological mechanism for the IWUE trend is a strong decrease in G_c as c_a rises. This finding challenges our capability to project vegetation responses to, and its feedbacks on, future climate and environmental change.

If such a strong physiological response occurred at the continental scale, it would entail significant impacts on hydrological and biotic processes on the land surface, especially when considering the fact that 55–67% of annual land water loss in temperate and boreal forests consists of transpiration (Schlesinger & Jasechko, 2014), that is, water that enters the atmosphere through stomata. Though changes in the regional water cycle and energy budget are hard to directly link to the physiological CO_2 effect experimentally, modeling studies using terrestrial biosphere models have demonstrated that land surface processes are sensitive to changes in G_c. Simulations showed that a CO_2-induced reduction in G_c triggers a reduction in ET, and consequently increases soil moisture, and continental runoff (Gedney *et al.*, 2006; Betts *et al.*, 2007; Cao *et al.*, 2010), as well as sensible heat flux and land surface temperature (Boucher *et al.*, 2009; Andrews *et al.*, 2011). Owing to the tight coupling of G_c and canopy photosynthesis, substantial large-scale changes in G_c are also likely to affect GPP and net biome productivity (NBP) at the regional to global scale, ecological processes which affect the concentration of atmospheric CO_2 and its seasonal amplitude (Randerson *et al.*, 1997; Forkel *et al.*, 2016).

Here we tested the plausibility of the strong increase in ecosystem IWUE from 1992 to 2010 as found by K13. We incorporated the assumed physiological driver of the trend, stomatal closure in response to rising atmospheric CO_2 concentrations, into the process-based terrestrial biosphere model JSBACH (Reick *et al.*, 2013), thereby forcing the observed trend in the model. The implications of the increased IWUE trend to carbon and water cycling at the continental scale were subsequently investigated by comparing JSBACH simulations of ET, continental runoff, and the seasonal amplitude of atmospheric CO_2 across the extratropical northern hemisphere with observation-based ET products (Mueller *et al.*, 2013), runoff measurements at major rivers, and observed atmospheric CO_2 concentrations across ground-based monitoring sites.

Material and Methods

JSBACH model description

The JSBACH model (Reick *et al.*, 2013; Knauer *et al.*, 2015; version 3.10, revision 687) is the land component of the MPI Earth System Model (Giorgetta *et al.*, 2013). Moisture, energy, and momentum fluxes between the land surface and the lower atmosphere are simulated using classical bulk transfer relations, in which aerodynamic land–atmosphere coupling is based on the Monin–Obukhov similarity theory (Roeckner *et al.*, 2003). Simulated evapotranspiration (ET) comprises transpiration by vegetation, soil evaporation, and evaporation of intercepted water, all of which are affected by seasonally varying vegetation cover and leaf area. Soil hydrological processes are represented in a five-layer scheme (Hagemann & Stacke, 2014). Surface runoff and drainage enter a river routing scheme which simulates lateral water fluxes on the land surface (HD model) (Hagemann & Dümenil, 1998). Vegetation in the model is represented as plant functional types (PFTs), which differ in their biochemical and biophysical attributes. Radiative transfer in the canopy is based on the two-stream approximation (Sellers, 1985). C3 photosynthesis is simulated according to the model by Farquhar *et al.* (1980) and stomatal conductance (g_s) is calculated with the Ball–Berry equation (Ball *et al.*, 1987):

$$g_s = g_0 + g_1 \frac{A_n \mathrm{rH}}{c_a}, \qquad \text{Eqn 1}$$

where A_n is net assimilation (mol m^{-2} s^{-1}), rH is relative humidity (−), and c_a is atmospheric CO_2 concentration (mol mol^{-1}). g_0 (0.005 mol m^{-2} s^{-1}) and g_1 (9.3) are fitted parameters, which

are kept constant across all C3 vegetation types and which represent the minimum stomatal conductance in darkness, and the sensitivity of g_s to A_n, respectively. Leaf-level values of A_n, g_s, and c_i are iteratively solved for three canopy layers, and scaled to their bulk canopy equivalents (GPP, G_c, C_i) with LAI.

Sensitivity of WUE to atmospheric CO_2 concentration

According to the Ball–Berry model (Eqn 1), iWUE (A_n/g_s) changes in proportion to c_a if rH and g_1 are assumed to remain unchanged with increasing c_a and $g_0 = 0$. In this case, a fractional change in c_a is expected to lead to the same fractional change in iWUE. This proportionality diminishes with increasing $\eta = g_0/g_s$, the fraction of g_s functionally not under guard cell control of the stomata and therefore not responding to an increase in c_a in the Ball–Berry model:

$$\frac{\mathrm{diWUE}}{\mathrm{iWUE}} = (1-\eta)\frac{\mathrm{d}c_a}{c_a}. \qquad \text{Eqn 2}$$

At the ecosystem level, the sensitivity of WUE to c_a diminishes further as a result of two main factors: partial decoupling of the canopy from the atmosphere; and water fluxes other than transpiration (i.e. soil evaporation and interception). The strength of canopy–atmosphere decoupling depends on the ratio of aerodynamic conductance (G_a) to G_c, and was quantified as the dimensionless decoupling coefficient Ω (Jarvis & McNaughton, 1986), which ranges from 0 (perfectly coupled) to 1 (completely decoupled):

$$\Omega = \frac{\varepsilon + 1}{\varepsilon + 1 + G_a/G_c}, \qquad \text{Eqn 3}$$

where ε is the change of latent heat content relative to the change of sensible heat content of saturated air. An important implication of this concept is that with increasing Ω, the physiological control of transpiration by stomata is reduced:

$$\frac{\mathrm{d}T}{T} = (1-\Omega)\frac{\mathrm{d}G_c}{G_c}. \qquad \text{Eqn 4}$$

That means a given fractional change in G_c leads to a weaker fractional change in T, with the attenuation being determined by the value of Ω. In addition, soil evaporation and interception are not directly affected by changes in G_c. Consequently, the sensitivity of WUE to c_a decreases with increasing fraction of soil evaporation and interception on the total ecosystem water loss (ϕ). Accounting for these factors, and assuming that Ω does not affect plant carbon uptake, the relation between ecosystem WUE (GPP/ET) and c_a can be written as:

$$\frac{\mathrm{dWUE}}{\mathrm{WUE}} = (1-\eta)(1-\Omega)(1-\phi)\frac{\mathrm{d}c_a}{c_a}. \qquad \text{Eqn 5}$$

It can be seen from Eqns 2 and 5 that WUE is not exactly proportional to an increase in c_a and that the responsiveness further decreases with increasing scale from leaf to ecosystem. Inserting typical values of η, Ω, and ϕ (see Supporting Information Table S1; Fig. S1) in Eqn 5 suggests that the sensitivity of WUE at ecosystem level is reduced compared with that at leaf level by *c.* 30% (Fig. S1).

Simulating increased stomatal sensitivity to atmospheric CO_2 concentration

To incorporate a stronger WUE response to c_a into the JSBACH model, we modified the Ball–Berry equation (Eqn 1) such that g_s shows an increased sensitivity to c_a:

$$g_s = g_0 + g_1\frac{A_n \mathrm{rH}}{c_a}\frac{1}{\max(1, 1+\xi((c_a - c_{a,\mathrm{base}})/c_{a,\mathrm{base}}))}, \qquad \text{Eqn 6}$$

where ξ is a constant stomatal sensitivity factor to c_a, and $c_{a,\mathrm{base}}$ is the baseline atmospheric CO_2 concentration, set to the value observed in 1992 (355.37 ppm), the beginning of the eddy covariance observations analyzed by K13. This formulation translates into a stronger stomatal response to CO_2 if c_a exceeds $c_{a,\mathrm{base}}$, with the strength of the response determined by ξ. In this case, the following relation can be established at the ecosystem level:

$$\frac{\mathrm{dWUE}}{\mathrm{WUE}} = (1-\eta)(1-\Omega)(1-\phi)\frac{\mathrm{d}\left(c_a + \xi\frac{c_a^2 - c_{a,\mathrm{base}}c_a}{c_{a,\mathrm{base}}}\right)}{\left(c_a + \xi\frac{c_a^2 - c_{a,\mathrm{base}}c_a}{c_{a,\mathrm{base}}}\right)}. \qquad \text{Eqn 7}$$

The sensitivity factor ξ was estimated for each site by numerically solving Eqn 7 using simulated site values of η, Ω, and ϕ (see Table S1), such that dWUE/WUE corresponded to the median annual trend observed by K13 (2.3% yr^{-1}). Note that Eqn 6 has no purpose other than increasing the stomatal sensitivity in the model, thereby causing IWUE to rise at a similar rate as reported by K13.

Model setup and analysis

We conducted two main simulations: a standard run (ST) with the original Ball–Berry stomatal model (Eqn 1) and a CO_2-sensitive run (SE) with an increased stomatal sensitivity to c_a from 1992 onwards (Eqn 6). Both model versions were run at ecosystem level for eddy covariance sites within the FLUXNET network, and also globally at T63 spatial resolution (*c.* 1.875° × 1.875°). The focus of the analysis was on forested regions in the extratropical northern hemisphere during the period 1992–2010, consistent with the analysis conducted by K13.

Two different meteorological reanalysis datasets were used to force the JSBACH model – CRUNCEP v.6 (http://dods.extra.cea.fr/data/p529viov/cruncep/readme.htm) and WFDEI (Weedon *et al.*, 2014) – which provide air temperature, precipitation, specific humidity, longwave and shortwave radiation, and surface wind speed at subdaily resolution. All forcing variables were brought to half-hourly resolution. Atmospheric CO_2

concentration was provided globally at annual resolution as specified in Le Quéré *et al.* (2015). Land cover was prescribed from the HYDE 3.1 historical land-cover inventory (Klein Goldewijk *et al.*, 2011), combined with the SYNMAP vegetation map (Jung *et al.*, 2006).

Site-level simulations

We performed site-level simulations at 21 FLUXNET sites to test the effects of the modified physiology on simulated IWUE. The sites correspond to those investigated by K13 and comprise deciduous broadleaf and evergreen needle-leaf forest ecosystems in the temperate and boreal zones. Site characteristics relevant for this study are listed in Table S1. We used reanalysis climate forcing rather than meteorological forcing from the towers to have continuous simulations for all sites over the entire 1992–2010 period, which was not available from the FLUXNET database. For overlapping years, the meteorology measured at the flux towers is in relatively good agreement with the one from the reanalyses (Fig. S2), but shows stronger trends in rH (Fig. S3). All climate variables were extracted from the pixel of the climate forcing fields (at original 0.5° resolution) where the respective site was located. For each meteorological data set, two runs were conducted, which served to attribute changes in IWUE to either c_a or other climate variables: all climate variables held constant (i.e. an average site year with respect to precipitation, temperature, and air humidity was repeated throughout the entire simulation period) but c_a allowed to vary; and all climate variables, including c_a, allowed to vary. Basic plant physiological (e.g. maximum carboxylation rate) and structural (LAI, vegetation height) attributes, as well as basic soil parameters (e.g. soil depth, particle size distribution) were adjusted to observed or estimated values for each site, if available. Mean annual summertime IWUE at site level was calculated as follows:

$$\mathrm{IWUE} = \mathrm{Median}\left(\frac{\mathrm{GPP}\cdot\mathrm{VPD}}{\mathrm{ET}}\right), \qquad \text{Eqn 8}$$

where GPP ($\mathrm{gC\,m^{-2}\,s^{-1}}$), ET ($\mathrm{kg\ H_2O\,m^{-2}\,s^{-1}}$), and VPD (hPa) represent filtered half-hourly values in the summer months June, July, and August. Modeled data were filtered as described in K13 to exclude photosynthetically inactive time periods to avoid phenological effects as a result of possible shifts in the growing season. Days with precipitation and the following day were excluded to reduce the fraction of nontranspirational (i.e. not physiologically controlled) water fluxes on ET. Annual summertime IWUE trends were estimated with the Theil–Sen single median method.

To investigate whether the simulated IWUE trends are sensitive to the representation of canopy photosynthesis in the model, we tested two alternative model versions at site level, one in which photosynthesis is calculated separately for sunlit and shaded canopy fractions (Spitters, 1986; denoted as 'sunlit_shaded' run), and one in which photosynthesis and g_s were explicitly coupled to the energy balance ('leaf_EB' run), in contrast to the version used in this study, which assumed equal canopy surface and air temperatures.

Continental simulations and evaluation datasets

For the global runs, the model was brought into equilibrium with respect to its water and carbon cycle using preindustrial climate forcing, atmospheric CO_2 concentration, and land use. We then ran the model with a transient forcing from 1860 to 2010 and with annually updated land cover. The sensitivity factor ξ for the continental runs was set to the mean value of all sites ($\xi = 7.6$).

Simulated monthly ET was compared with the diagnostic datasets and reanalyses of the LandFlux-EVAL multi-dataset synthesis (Mueller *et al.*, 2013), which were aggregated to the resolution of the model via conservative remapping. The analysis was restricted to regions north of 35°N and where forest cover (based on SYNMAP) exceeds 30%. Daily river discharge time series were downloaded from the Global Runoff Data Centre (GRDC; Koblenz, Germany: http://www.bafg.de/GRDC/EN/02_srvcs/21_tmsrs/riverdischarge_node.html) and aggregated to mean annual discharges. Missing years were filled with the mean of the respective time series. Rivers with more than 3 years missing from 1992 to 2010 were discarded. Data from 42 river-gauging stations in America (21) and Eurasia (21), whose river catchments cover *c.* 19.8 Mio $\mathrm{km^2}$, were used for the analysis (Table S2; Fig. S4).

The seasonal amplitude of atmospheric CO_2 from 1985 to 2010 was simulated using the atmospheric transport model TM3 (Rödenbeck *et al.*, 2003) in Jacobian representation (Kaminski *et al.*, 1999). Input to the TM3 model comprises global net biome productivity (NBP) from the JSBACH simulations, fossil fuel emissions (CDIAC, Boden *et al.*, 2013), and net ocean carbon fluxes from the Global Carbon Project (Le Quéré *et al.*, 2015). Simulated CO_2 amplitudes were compared with estimates from flask and continuous measurements collected by various institutions (see Rödenbeck, 2005). We selected six remote measurement stations (Table S3) whose seasonal cycle is predominantly influenced by the terrestrial biosphere north of 35°N (Randerson *et al.*, 1997). Both observed and simulated seasonal CO_2 amplitudes were calculated based on monthly averaged CO_2 time series as the difference between the maximum and the minimum atmospheric CO_2 concentrations in each calendar year, and normalized to the 1985–1991 reference period. Normalized amplitude trends and their uncertainties were calculated using linear mixed-effects models with station as random effect.

Results

Site-level simulations

The effects of the modified model formulation on simulated vegetation physiology, GPP, ET and WUE at site level are shown in Fig. 1 (for WFDEI forcing; see Fig. S5 for CRUNCEP forcing). Results from the CO_2-sensitive (SE) model formulation start to differ from those of the standard (ST) version after 1992, when c_a

New Phytologist

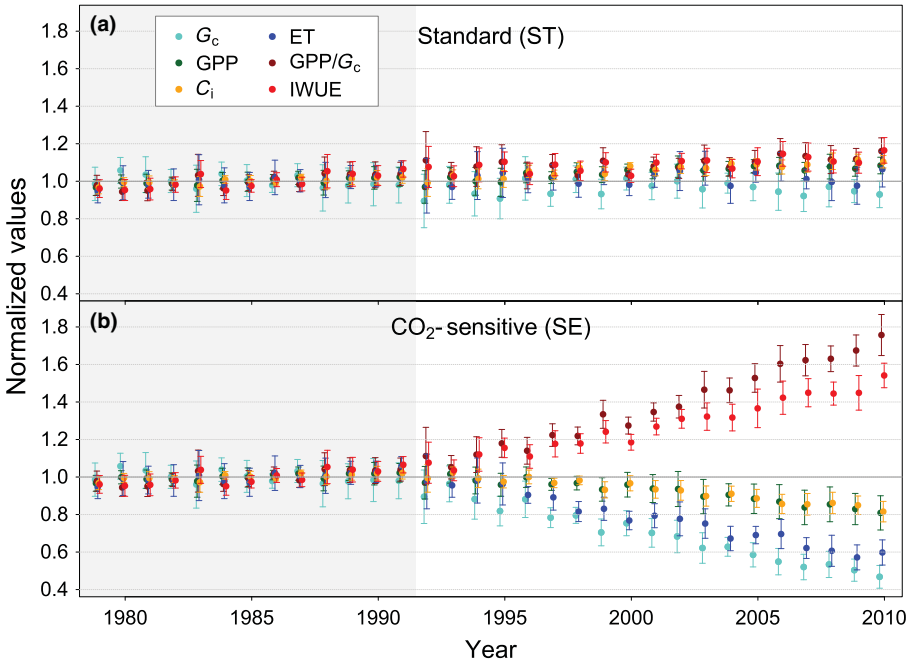

Fig. 1 Mean daytime summer (JJA) values (± SD) of canopy conductance (G_c), gross primary production (GPP), intercellular CO_2 concentration (C_i), evapotranspiration (ET), GPP/G_c, and inherent water-use efficiency (IWUE = (GPP × VPD)/ET) for: (a) the standard (ST) run; and (b) the CO_2-sensitive (SE) run. All variables are normalized to the mean of the 1979–1991 period (gray shaded area). Shown are results for WFDEI climate forcing (see Supporting Information Fig. S5 for CRUNCEP climate forcing). Values are averaged across the 21 eddy covariance sites.

exceeds $c_{a,base}$ (Eqn 6). Between 1992 and 2010, the higher CO_2 sensitivity in the SE run induces strong stomatal closure, which is apparent in the *c.* 53% reduction in g_s by the end of the simulation period (Fig. 1b). ET is reduced in parallel, but at an attenuated rate as a result of the contribution of nontranspirational water fluxes and canopy–atmosphere decoupling. The same holds true for IWUE when compared with the GPP/G_c response. In addition, C_i and GPP respond clearly to the partial stomatal closure and show a *c.* 20% reduction in 2010 compared with the reference period. The stronger decrease in ET compared with GPP leads to a strong increase in IWUE between 1992 and 2010 at all sites. Mean IWUE in 2010 exceeded that of the reference period by 54% and 60% for WFDEI and CRUNCEP forcing, respectively. The simulated increases in IWUE over all sites (median of 2.0% yr^{-1} for WFDEI and 2.2% yr^{-1} for CRUNCEP forcing, respectively) closely approach the annual IWUE increase of 2.3% yr^{-1} as observed by K13 (Fig. 2).

To attribute the changes in modeled IWUE to c_a or other climate variables, the simulated IWUE trends were compared between model runs forced with constant climate (CO_2 effect) and variable climate (both CO_2 and climate effects) in the ST model version. c_a caused a relatively constant contribution of *c.* 0.45% yr^{-1} to the IWUE trend across sites (Fig. 2), which agrees with the expected theoretical behavior and the formulation implemented in the model. All other climate variables reduced IWUE at some sites and enhanced it at others and thus introduced a large intersite variability to the IWUE trend (Fig. S6). However, the median across all sites remained almost constant for both CRUNCEP and WFDEI forcing (Fig. 2). Compared with the ST scenario,

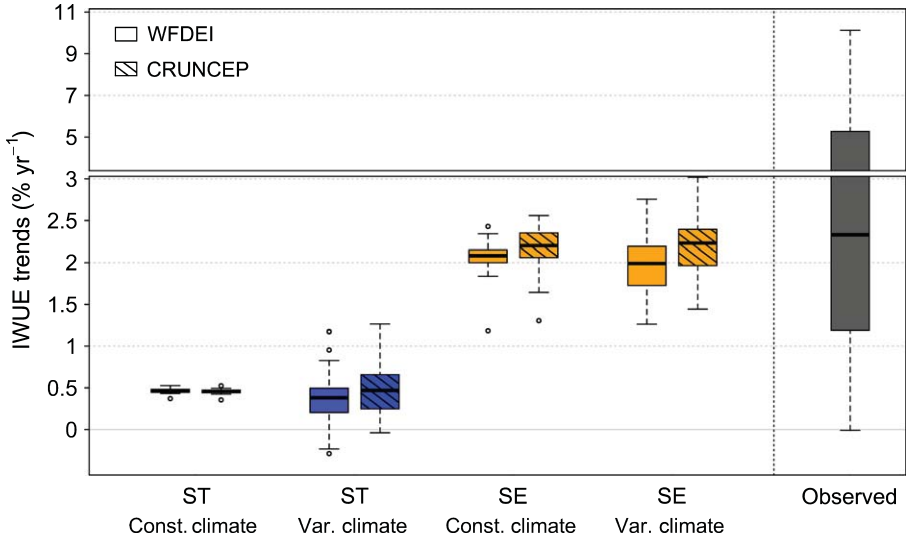

Fig. 2 Distribution of simulated inherent water-use efficiency (IWUE) trends (1992–2010) across all 21 flux tower sites for the standard (ST) and CO_2-sensitive (SE) runs with constant (Const.) climate, where all climate variables except atmospheric CO_2 concentrations were kept constant for an average site year, and variable (Var.) climate, where all climate variables, including atmospheric CO_2 concentrations, were allowed to vary. The boxes, bold horizontal lines, and circles indicate the interquartile ranges, medians, and data points outside 1.5 times the interquartile range, respectively. The right box depicts the corresponding observed trends reported by Keenan *et al.* (2013).

significantly higher IWUE trends were simulated in the SE scenario for all sites. SE runs with constant climate showed a similar IWUE response to the SE runs with variable climate (Fig. 2). These results suggest that the simulated IWUE trend in the SE version can be primarily attributed to CO_2 effects, and not to those of other climate variables (Fig. S7).

Simulated IWUE trends at site level in both alternative model versions ('sunlit_shaded' and 'leaf_EB') were in good agreement with the ones presented here (see Figs S8 and S9). An explicit coupling of photosynthesis and g_s to the energy balance as in the 'leaf_EB' run led to an increase in temperature and humidity at the canopy surface. However, these emerging meteorological gradients between the surface and the free air were constrained by the prescribed meteorological forcing and had little effect on the simulated IWUE trends.

WUE responses to atmospheric CO_2 concentration at leaf and ecosystem levels

Ecosystem WUE is less sensitive to rising c_a than its leaf-level equivalent, because factors such as nonstomatal water fluxes and aerodynamic resistance emerge at the ecosystem level that are negligible at the leaf level (Eqn 5). This scale dependency of the CO_2 sensitivity of WUE implies that an observed IWUE trend at ecosystem level is associated with a stronger iWUE trend at leaf level. To evaluate whether this affects the physiological interpretation of trends in ecosystem WUE, we performed idealized JSBACH simulations at the leaf and ecosystem levels using constant climate forcing to isolate the effects of increasing c_a (Fig. 3). The simulations at leaf and ecosystem levels were identical with respect to the calculation of photosynthesis and g_s (see Material

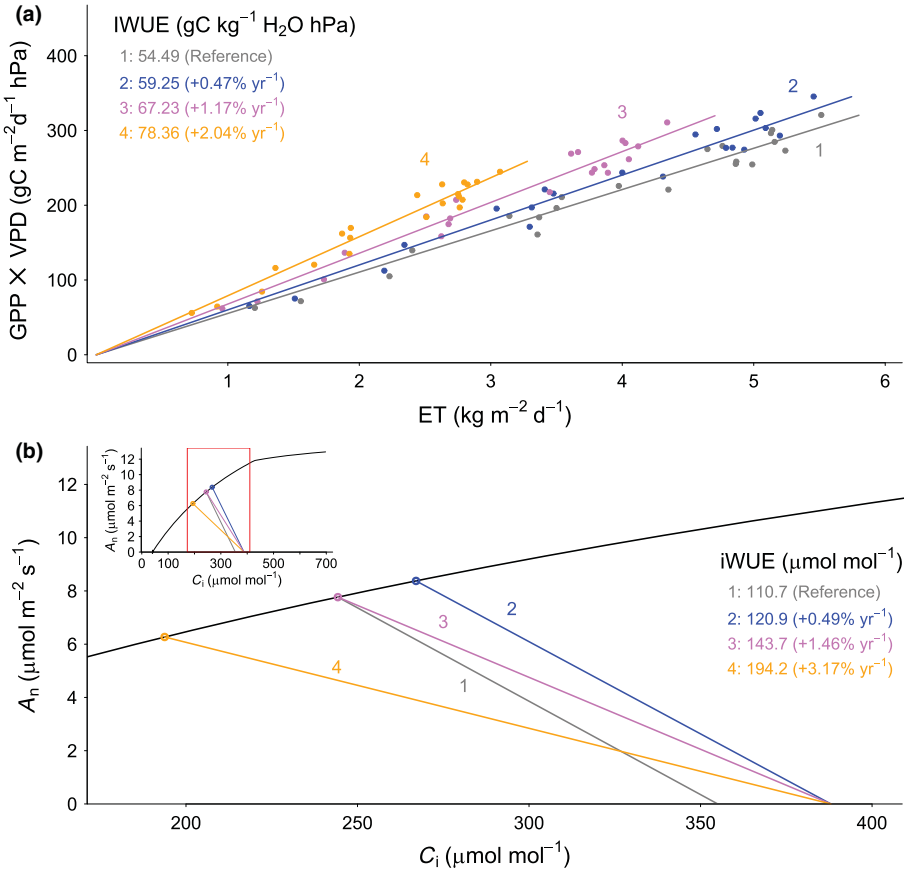

Fig. 3 (a) Simulated ecosystem inherent water-use efficiencies (IWUEs) and their trends for four runs differing in their stomatal response to atmospheric CO_2 concentration: (1) reference run: constant ratio of intercellular to atmospheric CO_2 concentrations (c_i/c_a) for c_a of 1992 (Ball–Berry); (2) constant c_i/c_a for c_a of 2010 (Ball–Berry); (3) constant c_i; and (4) stomatal closure inducing an IWUE increase of c. 2% yr^{-1}. Numbers on the left indicate simulated IWUEs (gC kg^{-1} H$_2$O hPa) in 2010, and their mean annual relative trends from 1992 to 2010 (in brackets). Each point represents one site and the slopes of the lines are across-site estimates of IWUE. IWUE was simulated by the JSBACH model, forced with WFDEI reanalysis, for the 21 FLUXNET sites characterized in Table S1. Non-CO_2 climate forcing was held constant in all runs. The following model settings were used for the respective simulations: (1) standard (ST) model version with c_a of 1992; (2) ST model version with c_a of 2010; (3) CO_2-sensitive (SE) model version with a mean sensitivity factor (ξ in Eqn 7) of 2.85 and c_a of 2010; (4) SE model version with a mean ξ of 7.6 and c_a of 2010. (b) The corresponding behavior at leaf level, simulated as in (a) but with a stand-alone version of the coupled photosynthesis-g_s model in JSBACH (Farquhar *et al.*, 1980; Ball *et al.*, 1987). The slope of the line originating at the abscissa is $-1/g_s$, and its intersection with the A_n/C_i curve ('operating point') gives the corresponding A_n and c_i values (Long & Bernacchi, 2003). Simulations were run with mean climate forcing from all sites (air temperature = 20.7°C, relative humidity = 52.7%, photosynthetically active photon flux density = 942 μmol m^{-2} s^{-1}) and with V_{cmax} = 40 μmol m^{-2} s^{-1}, J_{max} = 76 μmol m^{-2} s^{-1}, g_1 = 9.3, g_0 = 0.005 mol m^{-2} s^{-1} and with Rubisco kinetic parameters taken from Bernacchi *et al.* (2001).

and Methods), but the ecosystem-level simulations included scale-dependent feedbacks with the physical environment that are attenuated or nonexistent in the leaf-level simulations. We evaluated two common physiological scenarios with respect to stomatal responses to a rise in c_a (Saurer *et al.*, 2004): one in which stomatal closure leads to a constant c_i/c_a (as assumed by the Ball–Berry model), and one in which c_i remains constant over time (as proposed by K13, implying a somewhat stronger stomatal closure). Run 1 served as a reference and employed the Ball–Berry model (Eqn 1) with c_a as measured in 1992. According to the constant c_i/c_a scenario, the increase in c_a between 1992 and 2010 causes a slight decrease in g_s, and consequently a rise in iWUE, which is proportional to the change in c_a (run 2). Keeping c_i constant at the level of 1992 (run 3) requires an increased stomatal response to c_a which causes a larger iWUE trend between 1992 and 2010. In run 3, iWUE increases more than IWUE, which can be explained by the stronger impact of the attenuating factors (Eqn 5) at ecosystem level compared with leaf level. Importantly, the response associated with the constant c_i scenario is not sufficient to cause an IWUE trend in the magnitude as reported by K13 (median of 2.3% yr^{-1}; Fig. 2). To obtain an IWUE response similar to the one observed at the ecosystem level (run 4), the required physiological response at leaf level would need to involve a decrease in c_i over time.

Continental-scale implications of the observed IWUE trend

At the continental scale, the different physiological responses to c_a embedded in the ST and SE model versions are clearly reflected in ET, particularly in the summer months (Fig. 4a). The ST runs show a slight increase in ET across forested regions of the extratropical northern hemisphere from 1992 to 2005, which is in line with the reanalyses and the diagnostic ET products presented in Mueller *et al.* (2013). By contrast, the strong CO_2-induced decline in G_c in the SE scenario causes a significant decrease in ET, totaling *c.* 1% yr^{-1}, which is not in accordance with the

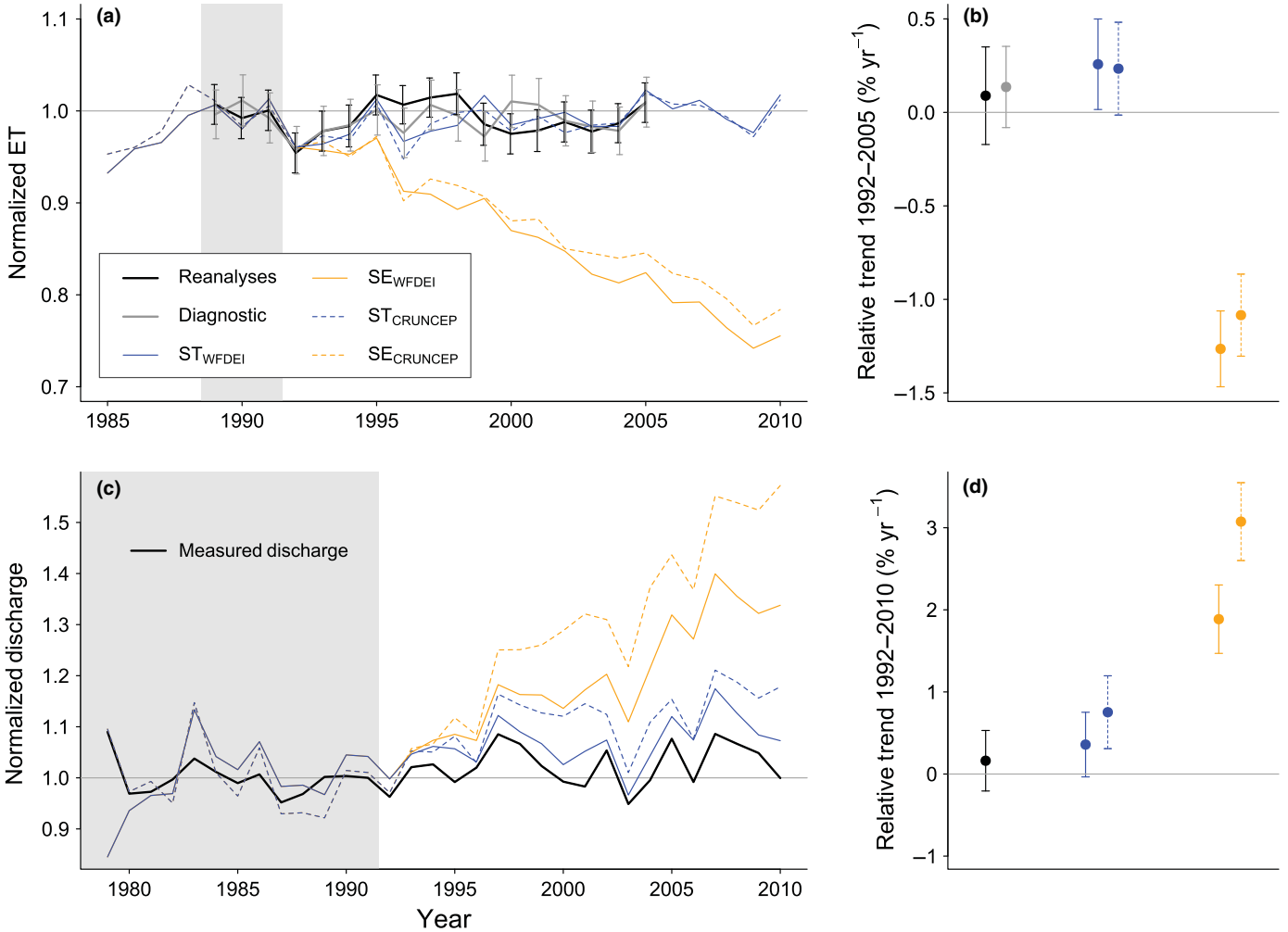

Fig. 4 (a) Normalized time series (gray shaded area: reference period 1989–1991) of observation-based (i.e. diagnostic and reanalysis products; see Mueller *et al.*, 2013) and simulated mean summer (JJA) evapotranspiration (ET). Error bars denote standard errors of the mean. (b) Confidence intervals for the trend in normalized ET from 1992 to 2005 based on ordinary least-squares (OLS) regression. (c) Normalized time series (reference period 1979–1991) of observed and simulated continental discharge, calculated as the sum of 42 individual river discharges. The location of the individual gauging stations and characteristics of the rivers are shown in Fig. S4 and Table S2, respectively. (d) Confidence intervals for the trend in normalized continental discharge from 1992 to 2010 based on OLS regression.

observation-based ET products (Fig. 4b). The choice of the climate forcing dataset had only minor effects on these results. The absolute mean summer values (Fig. S10a) demonstrate that simulated ET in the ST model version is underestimated compared with the data products and that their temporal dynamics are in moderate agreement (correlation coefficients (r) between 0.45 and 0.56). Although the ST and SE scenarios differ strongly, the difference between continental simulations was significantly lower than at site level as a result of the lower T/ET fraction in the absence of any data filtering, and the averaging across different vegetation types holding different aerodynamic properties.

A consequence of the modeled reduction in ET is an increase in simulated continental runoff (Fig. 4c,d). Across 42 river gauges (Table S2), normalized observed discharges show a slight, but not significant upward trend from 1992 to 2010. This behavior differs among rivers (Fig. S11). Simulated continental discharges in the ST versions are in agreement with the observations, but show stronger upward trends. The two SE model simulations show significantly higher discharge trends than both the ST runs and the observations (Fig. 4c,d). Both forcing products resulted in a good agreement of the modeled interannual variability with the observations ($r_{WFDEI} = 0.88$ and $r_{CRUNCEP} = 0.68$ for the 1992–2010 period). However, the use of WFDEI forcing yields more realistic absolute discharges (Fig. S10b) and weaker trends for the 1992–2010 time period than the CRUNCEP dataset. The strong underestimation of discharge (*c.* 40%) in simulations forced by the CRUNCEP dataset is indicative of a negative precipitation bias in this product, probably to some extent caused by the nonapplication of a precipitation undercatch correction (e.g. Biemans *et al.*, 2009).

The altered physiology in the SE model version had considerable implications for carbon cycling in the model. The strong stomatal closure affected vegetation carbon uptake (GPP) and NBP at large scales, which led to changes in the simulated seasonality of atmospheric CO_2 concentrations. Observations show an increase in the seasonal amplitude of atmospheric CO_2 concentrations in the northern hemisphere, corresponding to an intensified net carbon exchange across temperate and boreal terrestrial ecosystems (Graven *et al.*, 2013; Forkel *et al.*, 2016). The ST model runs simulated no changes to weak increases in the seasonal CO_2 amplitude at six ground-based measurement stations (Fig. 5). The SE runs, by contrast, showed significant decreasing trends, which are clearly unrealistic given the observations (Fig. 5). The progressive decrease in the CO_2 amplitude in the SE model version indicates a weakening of the seasonal carbon exchange in these ecosystems, which is caused by the marked decrease in GPP (Fig. S12) in response to the successively increasing stomatal limitations to photosynthesis.

To assess whether observed large-scale carbon and water fluxes are consistent with a constant C_i over time, we repeated the continental simulations using a model parameterization that yields a constant C_i at ecosystem level across FLUXNET sites (Eqn 6 with ξ set to 2.85). As expected, the resulting trends in ET, discharge, and atmospheric CO_2 amplitude showed an intermediate behavior between the ST and SE runs (Fig. S13). Nonetheless, this scenario is less consistent with the observations than the ST simulations, for all three observational datasets.

Discussion

WUE responses to atmospheric CO_2 concentration and other factors

Rising atmospheric CO_2 concentration is expected to increase plant WUE as a result of stomatal closure, but the exact magnitude of this effect is still under debate (e.g. Saurer *et al.*, 2004). Studies at the leaf to stand scale suggest stomatal closure commensurate with a constant c_i/c_a and iWUE at leaf level to rise in proportion to c_a ('constant c_i/c_a' scenario) (e.g. Ainsworth & Long, 2005; Frank *et al.*, 2015). The strong iWUE trend found by K13 has been attributed to the same physiological mechanism, but their results imply a much stronger stomatal response to c_a, which, as has been argued by K13, is consistent with an invariant C_i over time. Increasing the stomatal sensitivity to c_a in the JSBACH model resulted in increases in IWUE at site level that are similar to those observed by K13 from 1992 to 2010. However, the degree of stomatal closure necessary to cause this trend led to decreasing levels of C_i, GPP, and ET, which are

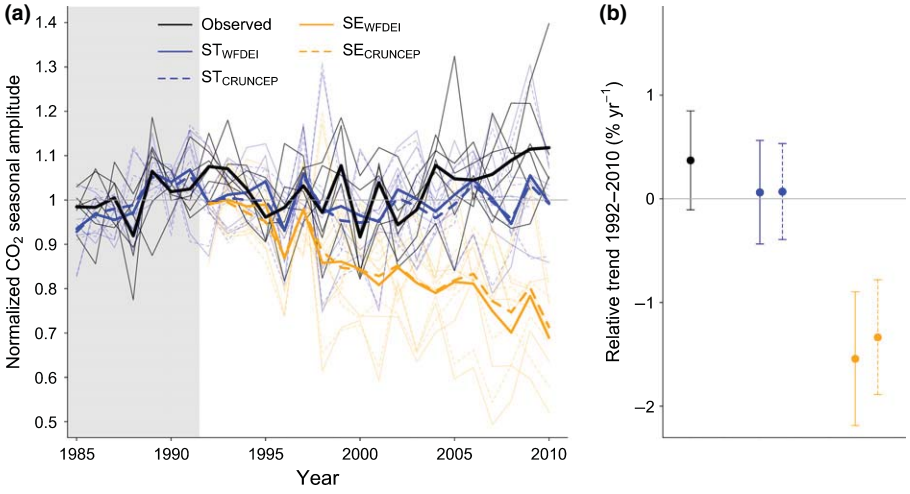

Fig. 5 (a) Individual (faint) and mean (bold) time series of normalized seasonal amplitudes of atmospheric CO_2 (gray shaded area: reference period), calculated as the difference between maximum and minimum CO_2 concentrations within a calendar year, based on six ground-based measurement stations (Table S3; Fig. S4). (b) Confidence intervals for the linear trends. Trends and confidence intervals were calculated using linear mixed-effects models assuming station as random effect.

inconsistent with observations from the eddy covariance sites. This implies that it is unlikely that CO_2-induced stomatal closure would have been the primary driving force behind the observed IWUE trend. Our simulations support previous empirical findings of a physiological regulation towards a constant c_i/c_a as c_a increases rather than a constant c_i (Fig. S13), and suggest a constant yet moderate contribution of c_a to the increase in IWUE, accounting for approximately one-quarter of the trend found by K13.

Besides atmospheric CO_2 concentration, other abiotic and biotic factors may have contributed to the trend. Climate change, for instance, has been found to influence WUE of grasslands and forests (De Boeck *et al.*, 2006; Yu *et al.*, 2008; Niu *et al.*, 2011), with the sign and magnitude of the response depending on the type of ecosystem and the prevailing climatic conditions (Tian *et al.*, 2010; Zhu *et al.*, 2011; Zhang *et al.*, 2014). Our model simulations at site level emphasize the strong climatic control on WUE. Climate factors other than c_a (e.g. VPD) enhanced, reduced, or, for some sites, reversed the positive effects of c_a on WUE in the ST scenario (Figs 2, S7). Additionally, changing biotic factors such as LAI can involve changes in WUE (Hu *et al.*, 2008; Zhang *et al.*, 2014). This and other biotic (e.g. canopy height) and abiotic (e.g. surface roughness) factors show no systematic changes over the study period and thus have been excluded as drivers for the WUE trend across sites by K13. Nevertheless, variables other than c_a may still have contributed to the IWUE trend nonuniformly across sites. The eddy covariance data used for the analysis by K13 might be subject to a sampling bias in space and, particularly, in time, considering that analyzed time series were as short as 7 yr for some sites. The magnitude of the trend found by K13 remains unexplained but might not be robust enough to draw conclusions on a 'mean' WUE response, representative across extratropical forest ecosystems, over the last two decades.

WUE definitions and their implications

Many different ways of calculating WUE have been proposed, depending on the scale and purpose of the investigation (see Kuglitsch *et al.* (2008) for an overview). For entire ecosystems, WUE is commonly defined as GPP/ET (e.g. Law *et al.*, 2002; Ponton *et al.*, 2006; Yu *et al.*, 2008; Huang *et al.*, 2015) and in some studies additional data screening is applied to ensure that ET represents mostly T (e.g. Ponton *et al.*, 2006). However, WUE calculated in this way is strongly influenced by the effects of VPD on ET (e.g. Law *et al.*, 2002; Ponton *et al.*, 2006; Tang *et al.*, 2014) with the consequence that observed dynamics in GPP/ET cannot be attributed to plant physiological function. To remove the confounding effects of VPD on WUE, an 'inherent' WUE (IWUE $= (\mathrm{GPP} \times \mathrm{VPD})/\mathrm{ET}$) has been proposed as a proxy of iWUE at the ecosystem level (Beer *et al.*, 2009). This formulation was adopted by subsequent studies. Recent considerations, however, have pointed out that the IWUE formulation neglects VPD effects on c_i/c_a (Zhou *et al.*, 2014), which decreases as a result of stomatal closure in response to rising VPD (e.g. Leuning, 1995). Based on the optimality theory (Cowan & Farquhar, 1977; Lloyd & Farquhar, 1994), Zhou *et al.* (2014) derived a new WUE metric termed 'underlying' WUE ($\mathrm{uWUE} = (\mathrm{GPP} \times \sqrt{\mathrm{VPD}})/\mathrm{ET}$), which they found to better capture the GPP–ET relationship. Importantly, uWUE and IWUE predict different WUE trends depending on the concomitant change in VPD (Fig. 6). As most sites investigated by K13 showed an increase in VPD over time (mean over all sites $\approx$ 1.25% yr^{-1}), the magnitude of the WUE trend would probably be smaller if calculated as uWUE, the physiologically more appropriate WUE metric. Considering the large effect of the WUE metric on the calculation of WUE trends as well as the central role ascribed to VPD in future climate change (Cook *et al.*, 2014), the choice of the WUE formulation is key when relating changes in WUE to plant physiological behavior.

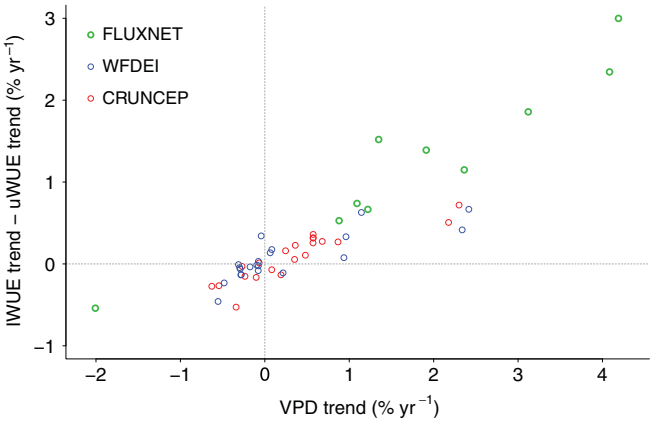

Fig. 6 Difference in water-use efficiency (WUE) calculated with different metrics (inherent WUE (IWUE) – underlying WUE (uWUE)) in dependence of a vapor pressure deficit (VPD) trend for observations from 10 FLUXNET sites and simulations for 21 FLUXNET sites forced with WFDEI and CRUNCEP reanalysis.

WUE response to atmospheric CO_2 concentration at leaf and ecosystem levels

Our considerations (Eqns 2–7) suggest that the sensitivity of WUE to c_a decreases with increasing scale from leaf to ecosystem, with the consequence that an observed CO_2 response of WUE at the ecosystem level corresponds to an even stronger physiological response within the leaves (Fig. 3). Thus, the required stomatal response at leaf level would have to involve a decline in c_i (Fig. 3), which is physiologically unlikely to happen (Saurer *et al.*, 2004). One reason for the difference across scales is aerodynamic conductance (G_a), which, depending on vegetation type and surface roughness, can exert strong control on canopy water use. The effect of G_a was discussed extensively by Jarvis & McNaughton (1986) in their 'omega' theory, which effectively describes the sensitivity of T to changes in G_c as a consequence of canopy–atmosphere decoupling. Ω calculated from micrometeorological measurements of G_a and derived G_c in temperate forests is usually in the range of 0.2–0.3 (e.g. Magnani *et al.*, 1998; Wullschleger *et al.*, 2000, 2002; Martin *et al.*, 2001). Modeled Ω by JSBACH (Table S1) was in accordance with field studies with a daytime mean of 0.21, indicating that the strength of the canopy–atmosphere decoupling is adequately represented in the model.

Not only does T tend to get less sensitive to c_a with increasing scale, but also G_c itself has been ascribed a lower responsiveness to c_a than its leaf-level equivalent g_s. Gunderson *et al.* (2002) and Wullschleger *et al.* (2002), for instance, found that stomata at lower canopy levels responded less to elevated c_a than those in the upper canopy. In the Ball–Berry model (Eqn 1), as in most other state-of-the-art stomatal models (e.g. Leuning, 1995; Medlyn *et al.*, 2011), the constant g_0 term reduces the sensitivity of g_s to c_a (Eqn 2) and further leads to a diminished response of G_c compared with g_s as a result of a larger g_0/g_s (η) fraction in lower canopy layers with lower photosynthetic rates. Given the firm physiological basis of g_0 and its importance for canopy transpiration (Barnard & Bauerle, 2013), its role in modeling G_c and WUE in ecosystem and land surface models deserves further investigation.

The analysis of IWUE usually relies on the assumption that ET consists almost entirely of T if an appropriate data filter is employed (see the Material and Methods section). This a critical assumption because nontranspirational water fluxes are not directly responsive to c_a and thus reduce the sensitivity of ecosystem water loss to rising atmospheric CO_2 concentrations, regardless of the physiological state of the vegetation. Our model simulations showed a low average residual contribution of evaporation of 4% across sites, indicating that the data screening applied here is sufficient to exclude water fluxes other than transpiration. It is worth mentioning that, in the absence of any data filter, evaporation and interception comprise a much larger fraction of ET (see Schlesinger & Jasechko, 2014), which leads to a considerably lower CO_2 effect on WUE over longer timescales (e.g. annually) (e.g. Wullschleger *et al.*, 2002; Leuzinger & Körner, 2007), which is also apparent in our continental-scale analyses.

Role of stomata in the hydrological response of the land surface to rising CO_2

At the continental scale, simulated ET showed a marked reduction in response to the strong stomatal closure in the SE scenario, which is in line with previous studies that have emphasized the high sensitivity of ET to G_c even at large spatial scales (Friend & Kiang, 2005; Gedney *et al.*, 2006). The implications of CO_2-induced stomatal closure on ET and the land surface energy budget, known as 'physiological forcing' (Betts *et al.*, 2007) is simulated in an exaggerated manner in the SE run, but shows qualitatively the same response as previous studies (Betts *et al.*, 2007; Boucher *et al.*, 2009; Cao *et al.*, 2010), including increases in continental runoff and land surface temperatures (but note Piao *et al.*, 2007).

One consequence of the reduced ET in the SE scenario was an increase in soil water content, a major indirect ecological effect of rising c_a (e.g. Morgan *et al.*, 2004). This effect plays only a minor role in this study as the focus was on regions where water limitation is of minor ecological importance. In water-limited regions, the simulated IWUE increase in the SE scenario is expected to be much weaker as a result of a positive feedback of increased water availability on vegetation productivity and thus ET.

In addition to its physiological effect through stomatal closure, rising c_a can affect vegetation structure through increases in biomass production and LAI (Cowling & Field, 2003). Experimental studies have reported increases in foliage cover in response to elevated c_a except for sites where the maximum leaf area carrying capacity has already been reached (Norby & Zak, 2011). This structural CO_2 effect through increased LAI is assumed to enhance transpiration and thus counteract the physiological CO_2 effect. However, its strength is poorly constrained and so are its implications for continental runoff (Gerten *et al.*, 2014). In simulation studies, the structural CO_2 effect was small in Betts *et al.* (2007), but considerable in other studies (Kergoat *et al.*, 2002; Bounoua *et al.*, 2010), and Piao *et al.* (2007) even identified an increase in runoff caused by c_a. The JSBACH model lacks a productivity–LAI feedback, which leads to an unchanged foliage cover throughout the simulation period despite clear changes in GPP. A more realistic representation of vegetation growth in the model would probably, to some extent, offset the simulated CO_2 response of both ET and GPP, leading to lower responses in continental runoff as well. In the ST runs, the simulated increase in discharge (Fig. 4c,d) may be partly attributed to the missing vegetation structure feedback in the model. Notwithstanding this, the trends in the SE run are strongly dominated by the pronounced simulated physiological effect (Fig. 2), which makes a strong compensatory effect of LAI unlikely in this model version.

Stomatal responses to atmospheric factors, including c_a and VPD, as well as the resulting ET are subject to multiple feedbacks at different scales (Field *et al.*, 1995; Wilson *et al.*, 1999; Vilà-Guerau de Arellano *et al.*, 2012), involving changes in the surface energy budget, temperature, convective boundary layer height, and cloud formation. The JSBACH model gives only a simplified representation of the mechanisms involved. In particular, the model was not coupled to the atmosphere, and thus any boundary layer feedbacks were precluded in the simulations. Although these additional feedbacks are assumed to stabilize the ET response at larger scales (Field *et al.*, 1995), a coupled model run would be necessary to test this assumption and to obtain a more complete representation of land–atmosphere interactions.

Does the observed ecosystem IWUE trend occur throughout the northern hemisphere?

The response of the terrestrial hydrological and carbon cycles to rising atmospheric CO_2 concentrations and their feedbacks on the climate system are key issues in climate change research (Gerten *et al.*, 2014). This work supports the majority of previous studies reporting moderate physiological responses of g_s and WUE to c_a at the plant scale compared with the recent suggestions by K13. The sensitivity of the total land–atmosphere water flux to the rise in c_a is further attenuated with increasing scale as a result of feedbacks with the physical environment. The combined implications of these two aspects are reflected in our results, which indicate that the magnitude of the ecosystem IWUE trend as reported by K13 is not in accordance with observed large-scale trends in continental discharge, ET, and the seasonal CO_2 exchange in temperate and boreal regions of the northern

hemisphere over the 1992–2010 time period (Figs 4, 5). The simulations demonstrate that changes in ecosystem IWUE in the magnitude as found by K13 would result, if they occurred at the continental scale, in altered carbon and water fluxes at the land surface that would be clearly detectable in signals responding to biogeochemical changes in the terrestrial biosphere. We thus conclude that the magnitude of the IWUE trend observed at temperate and boreal forest ecosystems is not a large-scale phenomenon.

Acknowledgements

This work used eddy covariance data acquired by the FLUXNET community (see Table S1; available at www.fluxdata.org) and, in particular, by the following networks: AmeriFlux (US Department of Energy, Biological and Environmental Research, Terrestrial Carbon Program (DE-FG02-04ER63917 and DE-FG02-04ER63911)), CarboEuropeIP, and Fluxnet-Canada (supported by CFCAS, NSERC, BIOCAP, Environment Canada, and NRCan). We acknowledge the financial support to the eddy covariance data harmonization provided by CarboEuropeIP, FAO-GTOS-TCO, iLEAPS, Max Planck Institute for Biogeochemistry, National Science Foundation, University of Tuscia, Université Laval and Environment Canada and US Department of Energy and the database development and technical support from Berkeley Water Center, Lawrence Berkeley National Laboratory, Microsoft Research eScience, Oak Ridge National Laboratory, University of California – Berkeley, University of Virginia. This study further uses the LandFlux-EVAL merged benchmark synthesis products of ETH Zurich produced under the aegis of the GEWEX and ILEAPS projects (http://www.iac.ethz.ch/url/research/LandFlux-EVAL/). S.Z. was supported by the European Research Council (ERC) under the European Union's H2020 programme (grant no. 647304; QUINCY). We are grateful to Steffen Richter, Kerstin Sickel and Christian Rödenbeck for technical assistance.

Author contributions

S.Z. and J.K. designed the study. J.K. performed the simulations and the analysis. S.Z., M.R., M.F., B.E.M., S.H. and C.W. contributed ideas to the analysis. J.K. wrote the manuscript, with contributions from all authors.

References

Ainsworth EA, Long SP. 2005. What have we learned from 15 years of free-air CO_2 enrichment (FACE)? A meta-analytic review of the responses of photosynthesis, canopy properties and plant production to rising CO_2. *New Phytologist* **165**: 351–372.

Ainsworth EA, Rogers A. 2007. The response of photosynthesis and stomatal conductance to rising [CO_2]: mechanisms and environmental interactions. *Plant, Cell & Environment* **30**: 258–270.

Andrews T, Doutriaux-Boucher M, Boucher O, Forster PM. 2011. A regional and global analysis of carbon dioxide physiological forcing and its impact on climate. *Climate Dynamics* **36**: 783–792.

Ball JT, Woodrow IE, Berry JA. 1987. A model predicting stomatal conductance and its contribution to the control of photosynthesis under different environmental conditions. In: Biggins J, ed. *Progress in photosynthesis research*. Dordrecht, the Netherlands: Martinus Nijhoff Publishers, 221–224.

Barnard D, Bauerle W. 2013. The implications of minimum stomatal conductance on modeling water flux in forest canopies. *Journal of Geophysical Research: Biogeosciences* **118**: 1322–1333.

Beer C, Ciais P, Reichstein M, Baldocchi D, Law B, Papale D, Soussana J-F, Ammann C, Buchmann N, Frank D *et al.* 2009. Temporal and among-site variability of inherent water use efficiency at the ecosystem level. *Global Biogeochemical Cycles* **23**: GB2018.

Bernacchi C, Singsaas E, Pimentel C, Portis A Jr, Long S. 2001. Improved temperature response functions for models of Rubisco-limited photosynthesis. *Plant, Cell & Environment* **24**: 253–259.

Betts RA, Boucher O, Collins M, Cox PM, Falloon PD, Gedney N, Hemming DL, Huntingford C, Jones CD, Sexton DM *et al.* 2007. Projected increase in continental runoff due to plant responses to increasing carbon dioxide. *Nature* **448**: 1037–1041.

Biemans H, Hutjes R, Kabat P, Strengers B, Gerten D, Rost S. 2009. Effects of precipitation uncertainty on discharge calculations for main river basins. *Journal of Hydrometeorology* **10**: 1011–1025.

Boden T, Marland G, Andres R. 2013. *Global, regional, and national fossil-fuel CO_2 emissions*. Oak Ridge, TN, USA: Carbon Dioxide Information Analysis Center, Oak Ridge National Laboratory, US Department of Energy.

Boucher O, Jones A, Betts RA. 2009. Climate response to the physiological impact of carbon dioxide on plants in the Met Office Unified Model HadCM3. *Climate Dynamics* **32**: 237–249.

Bounoua L, Hall F, Sellers P, Kumar A, Collatz G, Tucker C, Imhoff M. 2010. Quantifying the negative feedback of vegetation to greenhouse warming: a modeling approach. *Geophysical Research Letters* **37**: L23701.

Cao L, Bala G, Caldeira K, Nemani R, Ban-Weiss G. 2010. Importance of carbon dioxide physiological forcing to future climate change. *Proceedings of the National Academy of Sciences, USA* **107**: 9513–9518.

Cook BI, Smerdon JE, Seager R, Coats S. 2014. Global warming and 21st century drying. *Climate Dynamics* **43**: 2607–2627.

Cowan IR, Farquhar GD. 1977. Stomatal function in relation to leaf metabolism and environment. In: Jennings DH, ed. *Integration of activity in the higher plant*. Cambridge, UK: Cambridge University Press, 471–505.

Cowling SA, Field CB. 2003. Environmental control of leaf area production: implications for vegetation and land-surface modeling. *Global Biogeochemical Cycles* **17**: 1007.

De Boeck HJ, Lemmens C, Bossuyt H, Malchair S, Carnol M, Merckx R, Nijs I, Ceulemans R. 2006. How do climate warming and plant species richness affect water use in experimental grasslands? *Plant and Soil* **288**: 249–261.

De Kauwe MG, Medlyn BE, Zaehle S, Walker AP, Dietze MC, Hickler T, Jain AK, Luo Y, Parton WJ, Prentice IC *et al.* 2013. Forest water use and water use efficiency at elevated CO_2: a model-data intercomparison at two contrasting temperate forest FACE sites. *Global Change Biology* **19**: 1759–1779.

Doutriaux-Boucher M, Webb M, Gregory JM, Boucher O. 2009. Carbon dioxide induced stomatal closure increases radiative forcing via a rapid reduction in low cloud. *Geophysical Research Letters* **36**: L02703.

Ehleringer JR, Hall AE, Farquhar GD. 1993. *Stable isotopes and plant carbon–water relations*. San Diego, CA, USA: Academic Press.

Farquhar G, von Caemmerer S, Berry J. 1980. A biochemical model of photosynthetic CO_2 assimilation in leaves of C_3 species. *Planta* **149**: 78–90.

Feng X. 1999. Trends in intrinsic water-use efficiency of natural trees for the past 100–200 years: a response to atmospheric CO_2 concentration. *Geochimica et Cosmochimica Acta* **63**: 1891–1903.

Field C, Jackson R, Mooney H. 1995. Stomatal responses to increased CO_2: implications from the plant to the global scale. *Plant, Cell & Environment* **18**: 1214–1225.

Forkel M, Carvalhais N, Rödenbeck C, Keeling R, Heimann M, Thonicke K, Zaehle S, Reichstein M. 2016. Enhanced seasonal CO_2 exchange caused by amplified plant productivity in northern ecosystems. *Science* **351**: 696–699.

Frank D, Poulter B, Saurer M, Esper J, Huntingford C, Helle G, Treydte K, Zimmermann N, Schleser G, Ahlström A *et al.* 2015. Water-use efficiency and transpiration across European forests during the Anthropocene. *Nature Climate Change* **5**: 579–583.

Friend AD, Kiang NY. 2005. Land Surface Model development for the GISS GCM: effects of improved canopy physiology on simulated climate. *Journal of Climate* **18**: 2883–2902.

Gagen M, Finsinger W, Wagner-Cremer F, McCarroll D, Loader NJ, Robertson I, Jalkanen R, Young G, Kirchhefer A. 2011. Evidence of changing intrinsic water-use efficiency under rising atmospheric CO_2 concentrations in Boreal Fennoscandia from subfossil leaves and tree ring $\delta^{13}C$ ratios. *Global Change Biology* **17**: 1064–1072.

Gedney N, Cox P, Betts R, Boucher O, Huntingford C, Stott P. 2006. Detection of a direct carbon dioxide effect in continental river runoff records. *Nature* **439**: 835–838.

Gerten D, Betts R, Döll P (2014) Cross-chapter box on the active role of vegetation in altering water flows under climate change. In: Field CB, Barros VR, Dokken DJ, Mach KJ, Mastrandrea MD, Bilir TE, Chatterjee M, Ebi KL, Estrada YO, Genova RC *et al.*, eds. *Climate Change 2014: Impacts, Adaptation, and Vulnerability. Part A: Global and Sectoral Aspects. Contribution of Working Group II to the Fifth Assessment Report of the Intergovernmental Panel on Climate Change*. Cambridge, UK & New York, NY, USA: Cambridge University Press, 157–161.

Gerten D, Rost S, von Bloh W, Lucht W. 2008. Causes of change in 20th century global river discharge. *Geophysical Research Letters* **35**: L20405.

Giorgetta MA, Jungclaus J, Reick CH, Legutke S, Bader J, Böttinger M, Brovkin V, Crueger T, Esch M, Fieg K *et al.* 2013. Climate and carbon cycle changes from 1850 to 2100 in MPI-ESM simulations for the Coupled Model Intercomparison Project phase 5. *Journal of Advances in Modeling Earth Systems* **5**: 572–597.

Graven H, Keeling R, Piper S, Patra P, Stephens B, Wofsy S, Welp L, Sweeney C, Tans P, Kelley J *et al.* 2013. Enhanced seasonal exchange of CO_2 by northern ecosystems since 1960. *Science* **341**: 1085–1089.

Gunderson C, Sholtis J, Wullschleger S, Tissue D, Hanson P, Norby R. 2002. Environmental and stomatal control of photosynthetic enhancement in the canopy of a sweetgum (*Liquidambar styraciflua* L.) plantation during 3 years of CO_2 enrichment. *Plant, Cell & Environment* **25**: 379–393.

Hagemann S, Dümenil L. 1998. A parametrization of the lateral waterflow for the global scale. *Climate Dynamics* **14**: 17–31.

Hagemann S, Stacke T. 2014. Impact of the soil hydrology scheme on simulated soil moisture memory. *Climate Dynamics* **44**: 1731–1750.

Hu Z, Yu G, Fu Y, Sun X, Li Y, Shi P, Wang Y, Zheng Z. 2008. Effects of vegetation control on ecosystem water use efficiency within and among four grassland ecosystems in China. *Global Change Biology* **14**: 1609–1619.

Huang M, Piao S, Sun Y, Ciais P, Cheng L, Mao J, Poulter B, Shi X, Zeng Z, Wang Y. 2015. Change in terrestrial ecosystem water-use efficiency over the last three decades. *Global Change Biology* **21**: 2366–2378.

Jarvis PG, McNaughton K. 1986. Stomatal control of transpiration: scaling up from leaf to region. *Advances in Ecological Research* **15**: 1–49.

Jung M, Henkel K, Herold M, Churkina G. 2006. Exploiting synergies of global land cover products for carbon cycle modeling. *Remote Sensing of Environment* **101**: 534–553.

Kaminski T, Heimann M, Giering R. 1999. A coarse grid three-dimensional global inverse model of the atmospheric transport: 1. Adjoint model and Jacobian matrix. *Journal of Geophysical Research: Atmospheres* **104**: 18535–18553.

Katul G, Manzoni S, Palmroth S, Oren R. 2010. A stomatal optimization theory to describe the effects of atmospheric CO_2 on leaf photosynthesis and transpiration. *Annals of Botany* **105**: 431–442.

Keenan TF, Hollinger DY, Bohrer G, Dragoni D, Munger JW, Schmid HP, Richardson AD. 2013. Increase in forest water-use efficiency as atmospheric carbon dioxide concentrations rise. *Nature* **499**: 324–327.

Kergoat L, Lafont S, Douville H, Berthelot B, Dedieu G, Planton S, Royer J-F. 2002. Impact of doubled CO_2 on global-scale leaf area index and evapotranspiration: conflicting stomatal conductance and LAI responses. *Journal of Geophysical Research: Atmospheres* **107**: ACL-30.

Klein Goldewijk K, Beusen A, Van Drecht G, De Vos M. 2011. The HYDE 3.1 spatially explicit database of human-induced global land-use change over the past 12,000 years. *Global Ecology and Biogeography* **20**: 73–86.

Knauer J, Werner C, Zaehle S. 2015. Evaluating stomatal models and their atmospheric drought response in a land surface scheme: a multibiome analysis. *Journal of Geophysical Research: Biogeosciences* **120**: 1894–1911.

Kuglitsch F, Reichstein M, Beer C, Carrara A, Ceulemans R, Granier A, Janssens I, Koestner B, Lindroth A, Loustau D *et al.* 2008. Characterisation of ecosystem water-use efficiency of european forests from eddy covariance measurements. *Biogeosciences Discussions* **5**: 4481–4519.

Law B, Falge E, Gu Lv, Baldocchi D, Bakwin P, Berbigier P, Davis K, Dolman A, Falk M, Fuentes J *et al.* 2002. Environmental controls over carbon dioxide and water vapor exchange of terrestrial vegetation. *Agricultural and Forest Meteorology* **113**: 97–120.

Le Quéré C, Moriarty R, Andrew R, Canadell J, Sitch S, Korsbakken J, Friedlingstein P, Peters G, Andres R, Boden T *et al.* 2015. Global carbon budget 2015. *Earth System Science Data* **7**: 349–396.

Leuning R. 1995. A critical appraisal of a combined stomatal-photosynthesis model for C_3 plants. *Plant, Cell & Environment* **18**: 339–355.

Leuzinger S, Körner C. 2007. Water savings in mature deciduous forest trees under elevated CO_2. *Global Change Biology* **13**: 2498–2508.

Lloyd J, Farquhar GD. 1994. ^{13}C discrimination during CO_2 assimilation by the terrestrial biosphere. *Oecologia* **99**: 201–215.

Long S, Bernacchi C. 2003. Gas exchange measurements, what can they tell us about the underlying limitations to photosynthesis? Procedures and sources of error. *Journal of Experimental Botany* **54**: 2393–2401.

Magnani F, Leonardi S, Tognetti R, Grace J, Borghetti M. 1998. Modelling the surface conductance of a broad-leaf canopy: effects of partial decoupling from the atmosphere. *Plant, Cell & Environment* **21**: 867–879.

Martin T, Brown K, Kučera J, Meinzer F, Sprugel D, Hinckley T. 2001. Control of transpiration in a 220-year-old *Abies amabilis* forest. *Forest Ecology and Management* **152**: 211–224.

Medlyn BE, Duursma RA, Eamus D, Ellsworth DS, Prentice IC, Barton CV, Crous KY, de Angelis P, Freeman M, Wingate L. 2011. Reconciling the optimal and empirical approaches to modelling stomatal conductance. *Global Change Biology* **17**: 2134–2144.

Morgan J, Pataki D, Körner C, Clark H, Del Grosso S, Grünzweig J, Knapp A, Mosier A, Newton P, Niklaus PA *et al.* 2004. Water relations in grassland and desert ecosystems exposed to elevated atmospheric CO_2. *Oecologia* **140**: 11–25.

Morison JIL. 1987. Intercellular CO_2 concentration and stomatal response to CO_2. In: Zeiger E, Cowan I, Farquhar GD, eds. *Stomatal function*. Stanford, CA, USA: Stanford University Press, 229–251.

Mueller B, Hirschi M, Jimenez C, Ciais P, Dirmeyer P, Dolman A, Fisher J, Jung M, Ludwig F, Maignan F *et al.* 2013. Benchmark products for land evapotranspiration: LandFlux-EVAL multi-data set synthesis. *Hydrology & Earth System Sciences* **17**: 3707–3720.

Niu S, Xing X, Zhang Z, Xia J, Zhou X, Song B, Li L, Wan S. 2011. Water-use efficiency in response to climate change: from leaf to ecosystem in a temperate steppe. *Global Change Biology* **17**: 1073–1082.

Norby RJ, Zak DR. 2011. Ecological lessons from free-air CO_2 enrichment (FACE) experiments. *Annual Review of Ecology, Evolution, and Systematics* **42**: 181–203.

Peñuelas J, Canadell JG, Ogaya Ra. 2011. Increased water-use efficiency during the 20th century did not translate into enhanced tree growth. *Global Ecology and Biogeography* **20**: 597–608.

Piao S, Friedlingstein P, Ciais P, de Noblet-Ducoudré N, Labat D, Zaehle S. 2007. Changes in climate and land use have a larger direct impact than rising CO_2 on global river runoff trends. *Proceedings of the National Academy of Sciences, USA* **104**: 15242–15247.

Ponton S, Flanagan LB, Alstad KP, Johnson BG, Morgenstern K, Kljun N, Black TA, Barr AG. 2006. Comparison of ecosystem water-use efficiency among Douglas-fir forest, aspen forest and grassland using eddy covariance and carbon isotope techniques. *Global Change Biology* **12**: 294–310.

Randerson JT, Thompson MV, Conway TJ, Fung IY, Field CB. 1997. The contribution of terrestrial sources and sinks to trends in the seasonal cycle of atmospheric carbon dioxide. *Global Biogeochemical Cycles* **11**: 535–560.

Reick C, Raddatz T, Brovkin V, Gayler V. 2013. Representation of natural and anthropogenic land cover change in MPI-ESM. *Journal of Advances in Modeling Earth Systems* **5**: 459–482.

Rödenbeck C. 2005. *Estimating CO_2 sources and sinks from atmospheric mixing ratio measurements using a global inversion of atmospheric transport*. Jena, Germany: Max Planck Institute for Biogeochemistry Technical Reports 6.

Rödenbeck C, Houweling S, Gloor M, Heimann M. 2003. CO_2 flux history 1982–2001 inferred from atmospheric data using a global inversion of atmospheric transport. *Atmospheric Chemistry and Physics* **3**: 1919–1964.

Roeckner E, Bäuml G, Bonaventura L, Brokopf R, Esch M, Giorgetta M, Hagemann S, Kirchner I, Kornblueh L, Manzini E *et al.* 2003. *The atmospheric general circulation model ECHAM5. Part I: Model description.* MPI Reports, Max Planck Institute for Meteorology. Hamburg, Germany.

Saurer M, Siegwolf RT, Schweingruber FH. 2004. Carbon isotope discrimination indicates improving water-use efficiency of trees in northern Eurasia over the last 100 years. *Global Change Biology* **10**: 2109–2120.

Saurer M, Spahni R, Frank DC, Joos F, Leuenberger M, Loader NJ, McCarroll D, Gagen M, Poulter B, Siegwolf RT *et al.* 2014. Spatial variability and temporal trends in water-use efficiency of European forests. *Global Change Biology* **20**: 3700–3712.

Schlesinger WH, Jasechko S. 2014. Transpiration in the global water cycle. *Agricultural and Forest Meteorology* **189**: 115–117.

Sellers PJ. 1985. Canopy reflectance, photosynthesis and transpiration. *International Journal of Remote Sensing* **6**: 1335–1372.

Sellers PJ, Bounoua L, Collatz G, Randall D, Dazlich D, Los S, Berry J, Fung I, Tucker C, Field C *et al.* 1996. Comparison of radiative and physiological effects of doubled atmospheric CO_2 on climate. *Science* **271**: 1402–1405.

Spitters C. 1986. Separating the diffuse and direct component of global radiation and its implications for modeling canopy photosynthesis Part II. Calculation of canopy photosynthesis. *Agricultural and Forest Meteorology* **38**: 231–242.

Tang X, Li H, Desai AR, Nagy Z, Luo J, Kolb TE, Olioso A, Xu X, Yao L, Kutsch W *et al.* 2014. How is water-use efficiency of terrestrial ecosystems distributed and changing on Earth? *Scientific Reports* **4**: 7483.

Tian H, Chen G, Liu M, Zhang C, Sun G, Lu C, Xu X, Ren W, Pan S, Chappelka A. 2010. Model estimates of net primary productivity, evapotranspiration, and water use efficiency in the terrestrial ecosystems of the southern United States during 1895–2007. *Forest Ecology and Management* **259**: 1311–1327.

Vilà-Guerau de Arellano J, van Heerwaarden CC, Lelieveld J. 2012. Modelled suppression of boundary-layer clouds by plants in a CO_2-rich atmosphere. *Nature Geoscience* **5**: 701–704.

Waterhouse JS, Switsur V, Barker A, Carter A, Hemming D, Loader NJ, Robertson I. 2004. Northern European trees show a progressively diminishing response to increasing atmospheric carbon dioxide concentrations. *Quaternary Science Reviews* **23**: 803–810.

Weedon GP, Balsamo G, Bellouin N, Gomes S, Best MJ, Viterbo P. 2014. The WFDEI meteorological forcing data set: WATCH Forcing Data methodology applied to ERA-Interim reanalysis data. *Water Resources Research* **50**: 7505–7514.

Wilson KB, Carlson TN, Bunce JA. 1999. Feedback significantly influences the simulated effect of CO_2 on seasonal evapotranspiration from two agricultural species. *Global Change Biology* **5**: 903–917.

Wullschleger SD, Gunderson C, Hanson P, Wilson K, Norby R. 2002. Sensitivity of stomatal and canopy conductance to elevated CO_2 concentration-interacting variables and perspectives of scale. *New Phytologist* **153**: 485–496.

Wullschleger SD, Wilson KB, Hanson PJ. 2000. Environmental control of whole-plant transpiration, canopy conductance and estimates of the decoupling coefficient for large red maple trees. *Agricultural and Forest Meteorology* **104**: 157–168.

Yu G, Song X, Wang Q, Liu Y, Guan D, Yan J, Sun X, Zhang L, Wen X. 2008. Water-use efficiency of forest ecosystems in eastern China and its relations to climatic variables. *New Phytologist* **177**: 927–937.

Zhang F, Ju W, Shen S, Wang S, Yu G, Han S. 2014. How recent climate change influences water use efficiency in East Asia. *Theoretical and Applied Climatology* **116**: 359–370.

Zhou S, Yu B, Huang Y, Wang G. 2014. The effect of vapor pressure deficit on water use efficiency at the subdaily time scale. *Geophysical Research Letters* **41**: 5005–5013.

Zhu Q, Jiang H, Peng C, Liu J, Wei X, Fang X, Liu S, Zhou G, Yu S. 2011. Evaluating the effects of future climate change and elevated CO_2 on the water use efficiency in terrestrial ecosystems of China. *Ecological Modelling* **222**: 2414–2429.

Supporting Information

Additional Supporting Information may be found online in the Supporting Information tab for this article:

Fig. S1 Mean summer (JJA) values across all sites for η, Ω, and ϕ (Eqn 5) for WFDEI and CRUNCEP forcing.

Fig. S2 Mean summer (JJA) air temperature, precipitation, VPD, and relative humidity as measured at the eddy flux towers and in the reanalysis products.

Fig. S3 Relative trends of summer (JJA) air temperature and relative humidity at the eddy flux towers and in the reanalysis products.

Fig. S4 Location of FLUXNET sites, ground-based CO_2 measurement stations, and discharge gauging stations analyzed in this study.

Fig. S5 As Fig. 1, but with CRUNCEP climate forcing.

Fig. S6 IWUE trends (1992–2010) for all sites simulated with constant and variable climate in the standard (ST) model formulation, and for variable climate in the CO_2-sensitive (SE) model formulation.

Fig. S7 Contribution of climate variables other than atmospheric CO_2 concentration to the IWUE trend in the SE scenario.

Fig. S8 Results from an alternative model version, in which photosynthesis was calculated separately for sunlit and shaded fractions of the canopy.

Fig. S9 Results from an alternative model version, in which photosynthesis and stomatal conductance were explicitly coupled to the energy balance (EB).

Fig. S10 Mean summer ET of diagnostic and reanalysis products and mean annual discharges.

Fig. S11 Relative trends in measured and simulated discharge (with WFDEI climate forcing) for all rivers analyzed in this study.

Fig. S12 Time series of simulated GPP for the standard (ST) and CO_2-sensitive (SE) runs and WFDEI and CRUNCEP climate forcing, normalized to the 1985–1991 reference period.

Fig. S13 Confidence intervals for the trend in ET (as in Fig. 4b), continental discharge (as in Fig. 4d), and the seasonal CO_2 amplitude (as in Fig. 5b), including the 'constant C_i' scenario.

Table S1 Characteristics of flux tower sites used in this study

Table S2 Characteristics of rivers and associated discharge gauging stations used in this study

Table S3 List of CO_2 monitoring stations used in this study

Please note: Wiley Blackwell are not responsible for the content or functionality of any Supporting Information supplied by the authors. Any queries (other than missing material) should be directed to the *New Phytologist* Central Office.